

CHAPTER 3

NOISE ESTIMATION TECHNIQUES

3.1 INTRODUCTION

Noise level estimation plays an important role in image processing algorithms. In this chapter, several different approaches for noise level estimation are studied and discussed. The methods are studied in terms of accuracy, sensitivity to varying noise levels, and complexity. Two methods are implemented and used in later chapters.

In many image processing applications, such as image denoising, enhancement, compression, format conversion, etc., accurate knowledge of the noise level present in the input image is of crucial importance for tuning the parameters of the corresponding image processing algorithm. The precise information about the noise present in images can significantly impact the effectiveness of image processing algorithms and can be used for optimization of these algorithms (e.g., edge detection, segmentation, filtering, etc.), where the parameters of the algorithm are adapted to the noise level.

This chapter is organized as follows: in Section 3.2 the image noises are classified. The noise estimation techniques are explained in Section 3.3. In Section 3.4 we present experimental results and discussion of noise estimation techniques used in later chapter. The summary is given Section 3.5.

3.2 TYPES OF IMAGE NOISES

The image noise can be classified based on their characteristics [Vaseghi 2000]:

- Concerning different amplitude distributions of the noise- quantization noise (typically has a uniform distribution), thermal noise (has a Gaussian distribution) and quantum noise (which has a Poisson distribution).
- Concerning the statistical dependence of the noise level on the signal- signal dependent (e.g. multiplicative noise) noise and signal independent noise.
- Concerning the statistical dependence between the noise samples- correlated and non-correlated noise.
- Concerning the orientation dependence- the noise correlation properties may be different in the horizontal, the vertical direction.
- Concerning different frequency characteristics- white noise (uniform), 1/f noise and triangular noise.

In many image applications, the noise is well modeled by independent, identically distributed (i.i.d.), additive zero mean white Gaussian [Amer 2005]. We adopt this model and assume spatial stationarity unless it is explicitly stated otherwise. A noisy image is given as:

$$f'(x, y) = f(x, y) + n(x, y) \quad (3.1)$$

where $f(x, y)$ and $f'(x, y)$ stand for the noise-free image and noisy image with additive noise $n(x, y)$, respectively.

The independent identically distributed (i.i.d) Gaussian noise is added independently to the luminance value at each pixel position. The gray-scale Lena image with added white Gaussian noise is shown in Fig. 3.1. As can be noticed from Fig. 3.1, the noise is uniformly spread through the whole image but the noise is more visible in the flat image areas than in the textured areas.



(a) Original Lena Image (b) with added Gaussian noise

Fig. 3.1 Visual perception with additive white Gaussian noise

This comes from the fact that the human eye is more sensitive to the variations in the low frequency image components than in the high frequency components. The noise level present in image is estimated by measuring deviations in intensity that are not due to noise free image structure, i.e., to distinguish between the noise and spatial structure present in the image. The noise estimation techniques are classified based on method used in next section.

3.3 TYPES OF NOISE ESTIMATION TECHNIQUES

The noise level estimation methods can be classified as:

- Block-based methods- The estimated noise variance is taken as a function of the local variances within image blocks belonging to the most homogeneous area.
- Smoothing-based method- The differences of the noisy and the smoothed image pixels are assumed to correspond to the noise, and the noise level is estimated by taking into account the differences that are smaller than a predefined threshold.

- Gradient based method- The spatial gradients for the noisy image are evaluated and their statistical distribution is analyzed in order to estimate the noise level.
- Wavelet based method- The high frequency subband is considered as noise and its variance is calculated.

Some of the noise estimation approaches were evaluated and compared in [Olsen 1993] and [Rank 1999] where it was concluded that the approach, which is based on first suppressing image structures by pre-filtering and then computing the noise variance, provides the most reliable results for a wide range of noise levels and images with different content. In [Amer 2005] the intra-scale block-based method is applied to image and was shown to outperform the methods of [Olsen 1993]. On the other hand in the recent approach of [Stefano 2004] a gradient based method is compared to the wavelet-based median absolute deviation (MAD) noise estimator of Donoho and Johnstone [Donoho 1994].

The absolute difference error is considered as evaluation indices. The absolute difference is defined as:

$$E_i = |\hat{\sigma}_n - \sigma_n| \quad (3.2)$$

where $\hat{\sigma}_n$ and σ_n are estimated and the true standard deviation of noise n , respectively.

3.3.1 Block Based Noise Estimation

Block-based noise estimation techniques use only information from the image. One of the most common approaches for intra-image noise estimation is the block based approach, where the image is divided in a set of image blocks and the estimated noise variance is computed as a combination of the k smallest variances measured in the

corresponding blocks, where k is a small number [Amer 2005] and [Rank 1999]. Lee and Mastin had suggested a block-size of 7×7 pixels to ensure a robust estimation [Lee 1981] and [Mastin 1985]. It has been experimentally proven to be a good compromise between efficiency and effectiveness for many images [Olsen 1993]. Specifically, smaller window size potentially provides more reliable and efficient noise estimation results because of the lower possibility of image structures influence to the result, and less computation. This however, holds only for the low noise levels, while for the higher noise levels larger number of samples are needed for accurate (in absolute sense) noise level estimation because of the heavier tail of the noise distribution.

The estimated noise variance is computed from the average of the smallest variances in a set of image blocks, where the number of blocks used in the averaging operation is chosen as a fixed percentage p of the total number of blocks in an image [Lee 1981]. A similar but more sophisticated method is based on variable blocks size in a multi-resolution approach [Meer 1990]. Another block-based method computes the local noise level for each block B [Haan 1996], where the noisy image is divided into non-overlapping blocks $B(c)$, with c being the center of the block. The local noise level is determined as the mean absolute difference over a block:

$$MAD(c) = \frac{1}{M} \sum_{(x,y) \in B(c)} |f'(x,y) - (f'(x,y) - u)| \quad (3.3)$$

where u is a constant vector (usually unitary in horizontal direction) and M stands for the number of pixels in the block. Specifically, u is used for determining the spatial gradient in correspondence to the position (x, y) .

Similarly, in another approach, the image is first pre-filtered by a high-pass or band-pass filter and the sum of the absolute values of the processed pixel values in a block is

computed [Rank 1999]. The sum is computed within non-overlapping blocks. Finally, the average of the p smallest sums within a field is computed.

A somewhat different approach for block-based noise estimation, where the noise variance is estimated in three steps [Rank 1999]. In a first step, the noisy image is filtered by a horizontal and vertical difference operator to reduce the influence of the unknown noise-free image. In the second step, a histogram of local variances of the blocks in the image is computed. Finally, the histogram is statistically evaluated in order to obtain the noise variance estimate. Although the experimental results show good performance, the number of experiments, measures and comparison methods used were insufficient to show a significant improvement of the method over other related methods. Moreover, the success of the algorithm depends heavily on correct parameter tuning (e.g., the number of process iterations or the shape of the used fade-out cosine-based function to evaluate the variance histogram).

Another block-based approach of assumes that a percentage p of image blocks can be considered as homogeneous and as such can be used to estimate the noise level [Van De Villa 2003]. Namely, for each block B in the image, a rough measure for the homogeneity μ is computed by considering the maximum and the minimum pixel value:

$$\mu = 1 - \frac{\max_{(x,y) \in B} f'(x, y) - \min_{(x,y) \in B} f'(x, y)}{R} \quad (3.4)$$

where R stands for the number of grey levels (in our case $R = 255$). Next a histogram of the homogeneity values is computed and a percentile p of the most homogeneous blocks is determined. Finally, the value μ_p of this percentile p is related to the noise estimate $\hat{\sigma}_n$ by the linear relationship:

$$\hat{\sigma}_n = (I - \mu_p) \nu_L \quad (3.5)$$

where ν_L denotes the slope, which is determined empirically using large number of synthetic patches.

A block-based noise estimation method is proposed by Amer which used a new measure for determining intensity-homogeneous blocks and a new structure analyzer for rejecting blocks [Amer 2005]. First the image is divided into blocks B , which can be non-overlapping or overlapping (depending on the implementation). The uniformity analyzer is applied to each block B . This analyzer is based on high-pass operators that measure homogeneity in eight different directions for each pixel. For each direction the homogeneity measure ξ_B is computed as:

$$\xi_B = 2c - n_1 - n_2 \quad (3.6)$$

where the abbreviation c stands for the central pixel value and n_1 and n_2 stand for the two nearest (highlighted) neighboring pixel values in a given direction, as illustrated in Fig. 3.2. The absolute values of all eight homogeneity measures ξ_B (for eight different directions) are summed to give the final homogeneity measure ξ_B for the block B . The sample variances σ_B^2 of the p most homogeneous blocks B (with smallest ξ_B) are averaged in order to estimate the noise variance $\hat{\sigma}_n^2$:

$$\hat{\sigma}_n^2 = \frac{\sum_{k \in V} \sigma_{B_k}^2}{p} \quad (3.7)$$

where V being the set of the indexes of the p blocks with the smallest values of ξ_B .

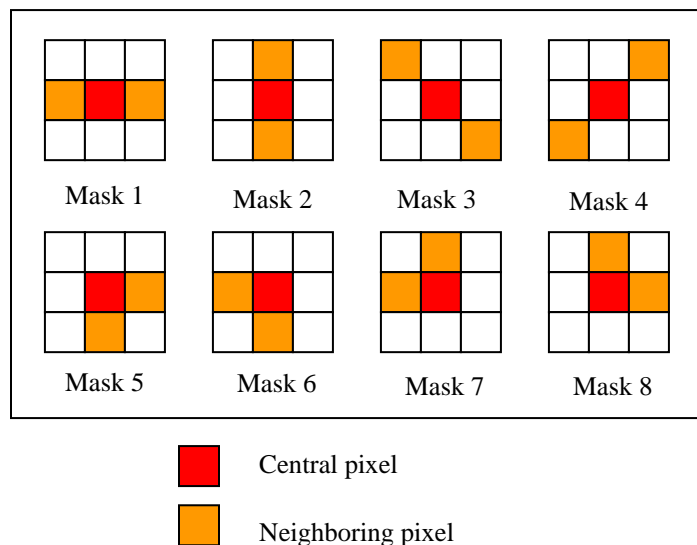


Fig. 3.2 Direction of the homogeneity analyzer for 3x3 blocks

To improve the performance of the method, only blocks that show similar homogeneity are included in the averaging process. Specifically, the median of homogeneity of the p smallest values of ξ_B is used as a reference value, for finding the most similar homogeneity values; the noise variance of the blocks with homogeneity values significantly different to the median value (above predefined threshold value) are excluded from the averaging. The results show that the algorithm outperforms the methods of [Olsen 1993] and [Rank 1999].

3.3.2 Gradient-based noise estimation

As opposed to block-based methods, which search for the “most uniform” image area and estimate the standard deviation in that region, gradient based methods extract the information about the noise variance from the most uniform area without searching for it [Gonzalez 2002]. The basic approach in gradient-based techniques is to extract the high frequency information and then evaluate the corresponding image

gradients in a specific way, in order to determine the estimated noise standard deviation $\hat{\sigma}_n$.

The method assumes that image structures like edges have strong second order differential components [Immerkaer 1996], which means that the Laplacian of an image is very sensitive to image structures. This suggests that by applying the difference operator of two masks L_1 and L_2 , each approximating the Laplacian operator, to the noisy input image one can obtain the output image that approximately corresponds to noise only. The proposed masks L_1 and L_2 used are:

$$L_1 = \begin{array}{|c|c|c|} \hline 0 & 1 & 0 \\ \hline 1 & -4 & 1 \\ \hline 0 & 1 & 0 \\ \hline \end{array} \quad L_2 = \begin{array}{|c|c|c|} \hline 1 & 0 & 1 \\ \hline 0 & -4 & 0 \\ \hline 1 & 0 & 1 \\ \hline \end{array}$$

and the difference operator N is defined as follows:

$$N = L_2 - 2L_1 = \begin{array}{|c|c|c|} \hline 1 & -2 & 1 \\ \hline -2 & 4 & -2 \\ \hline 1 & -2 & 1 \\ \hline \end{array}$$

where the operator N has zero mean and variance 36. Hence by applying the N operator to the input noisy image $f'(x, y)$, the variance of the noise can be estimated as:

$$\sigma_n = \frac{1}{36(W-2)(H-2)} \sum_{\text{Image}_n} (N * f'(x, y))^2 \quad (3.8)$$

where W and H stand for the width and height of the image, respectively. Note that by assuming that the standard deviation of noise at each pixel position in the noisy image

$f'(x, y)$ is σ_n , the variance of the $N f'(x, y)$ will be $36\sigma_n^2$. Consequently, the division by 36 is introduced in equation (3.8).

The gradient based method for noise estimation is based on the gradient distribution evaluation [Vorhees 1987]. The distribution of the spatial gradient magnitudes is evaluated from the noisy image. The gradient amplitudes $\|g\|$ are determined in terms of the horizontal and vertical gradient component values g_x and g_y , where $\|g\| = \sqrt{g_x^2 + g_y^2}$. The idea is that in case of an ideally uniform image with added white Gaussian noise, the two gradient components g_x and g_y are iid white Gaussian processes, thus yielding the Rayleigh distribution for the gradient magnitude $\|g\|$. However, for typical images, which

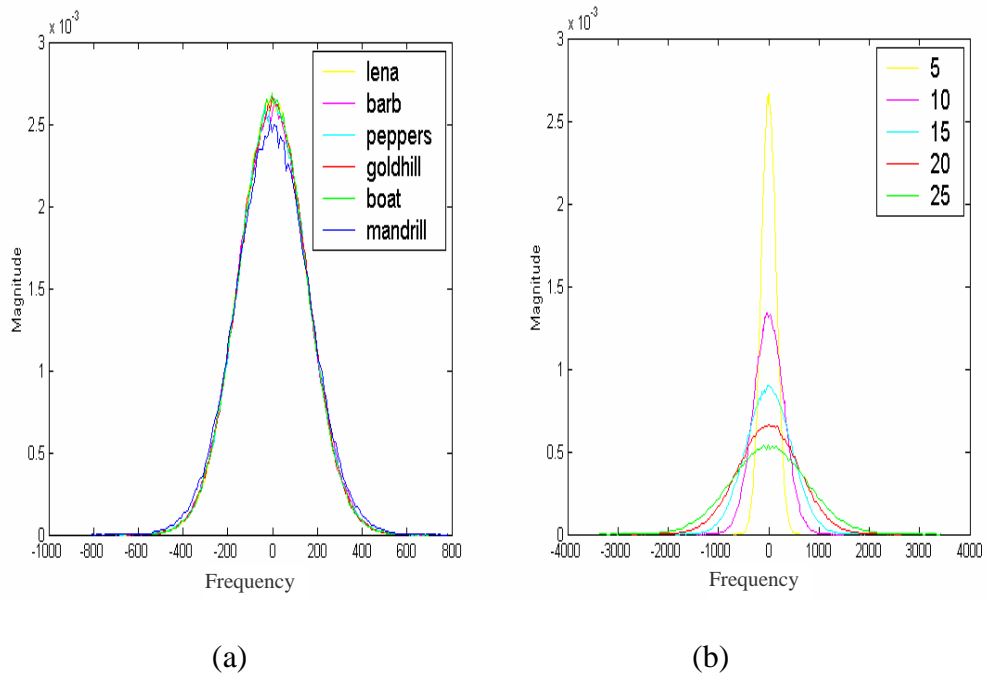


Fig. 3.3 Noise estimation (a) Normalized histogram of the gradient magnitudes with Gaussian noise. (b) Normalized histograms of the gradient magnitude for the Lena with different levels of the Gaussian noise.

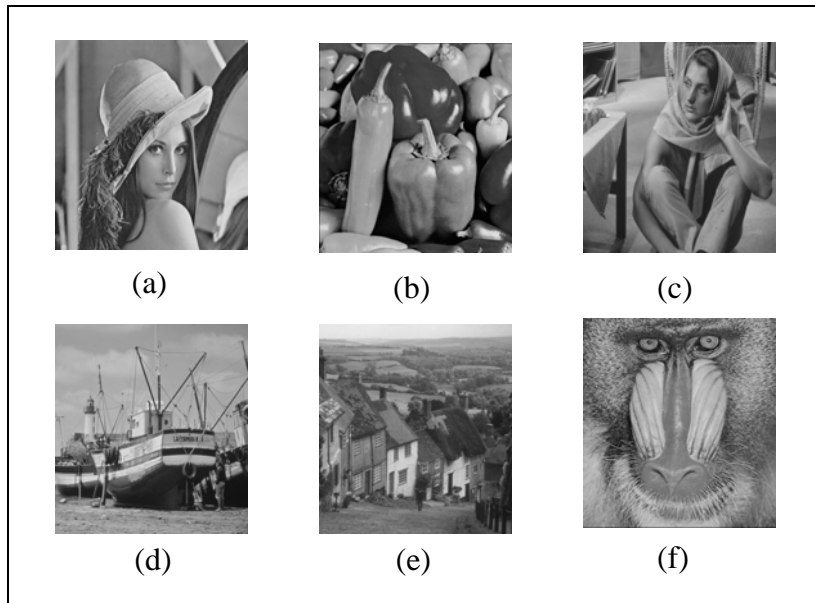


Fig. 3.4 The images used for the gradient Method (a) Lena (b) Peppers (c) Barbara (d) Boat (e) Goldhill (f) Baboon

are not ideally uniform, the actual distribution of the gradient magnitudes differs from the Rayleigh distribution, which consequently introduces errors in the noise estimation approach. In Fig. 3.3(a), we illustrate the normalized histograms of the spatial gradient magnitudes for the same noise level ($\sigma_n = 25$), for different images shown in Fig. 3.4. Note that in case of an ideally uniform image, the histogram is nothing else than the mode of the corresponding Rayleigh distribution, which in that case equals the standard deviation of the noise:

$$\sigma_n = \gamma \tag{3.9}$$

where γ denotes the most frequent gradient magnitude, which is only approximately the same for different images with different spatial content.

The more spatial content is present in the input noisy image, the more the histogram will deviate from the Rayleigh distribution. Specifically, the tail of the histogram may change significantly while the most frequent gradient amplitude will deviate to a smaller extent (shifts to the right), as can be observed from Fig. 3.4(a).

The normalized spatial gradient histograms of Lena image with different noise levels is shown in Fig. 3.4(b). It can be seen that the peak of the distribution (the most frequent gradient amplitude γ) shifts to the right for higher noise levels, hence allowing to measure the noise level by tracking γ . However, the deviation of the shape of the gradient histogram from the corresponding Rayleigh distribution is not the same for all noise levels and consequently the magnitude of shift to the right differs also for different noise levels. Specifically, for lower noise levels ($\sigma_n = 5$) the histogram deviates more from the Rayleigh distribution than for higher noise levels (see Fig. 3.4(b)). This is because at higher noise levels the gradient distribution becomes dominated by noise and is less sensitive to the noise-free image content.

The other method based on distribution of the gradient magnitudes is proposed by [Zlokolica 2004]. The noise estimators are using information from the spatial gradients. The gradients are obtained by a small-scale operator. This is because large-scale operators [Sonka 1999] are found to increase the sensitivity of the noise estimation approach to image details and reduce the accuracy of the noise estimates in comparison to the case when a small-scale operator are used. The noise estimator is based on evaluating the distribution of spatial gradient magnitudes. The histogram of the gradient magnitudes is plotted and seeks the correspondence between the most frequent gradient magnitude and the estimated noise standard deviation. Specifically, the optimal correspondence

between the gradient value at which the gradient histogram peaks (most frequent gradient) and the estimated standard deviation of noise, in the least squares sense, across the training set of images and for all noise levels. The gradients are computed using the Sobel operator [Sonka 1999], which is computed as the square root of the derivatives in horizontal g_x and vertical g_y directions. The corresponding operator used, consists of a pair of 3×3 convolution kernels as shown in Fig. 3.5 The output of the Sobel operator, i.e., the magnitude gradient, for the discrete spatial position (x, y) , is given by:

$$G(x, y) = \sqrt{(f'(x, y) * \Delta_x)^2 + (f'(x, y) * \Delta_y)^2} \quad (3.10)$$

$$= \sqrt{g_x^2(x, y) + g_y^2(x, y)}$$

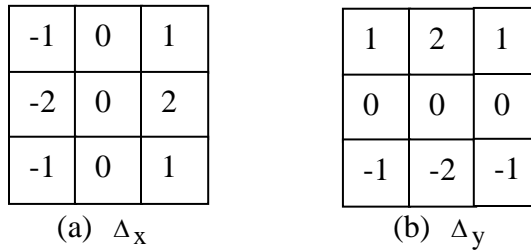


Fig. 3.5 Kernels for horizontal and vertical edge detection in the Sobel operator

Let h denote the histogram of $G(x, y)$ for the image over all discrete spatial positions (x, y) . The most frequent gradient from the input image, i.e., the abscissa value γ at which the amplitude gradient histogram h peaks, as follows:

$$\gamma = \underset{i \in Q}{\operatorname{argmax}}(h(i)) \quad (3.11)$$

Fig. 3.6(a) and Fig. 3.6(b) show the noisy “Boat” image (Gaussian noise, $\sigma_n = 10$) and its Sobel processed image, respectively. The gradient histogram of the “Boat” image

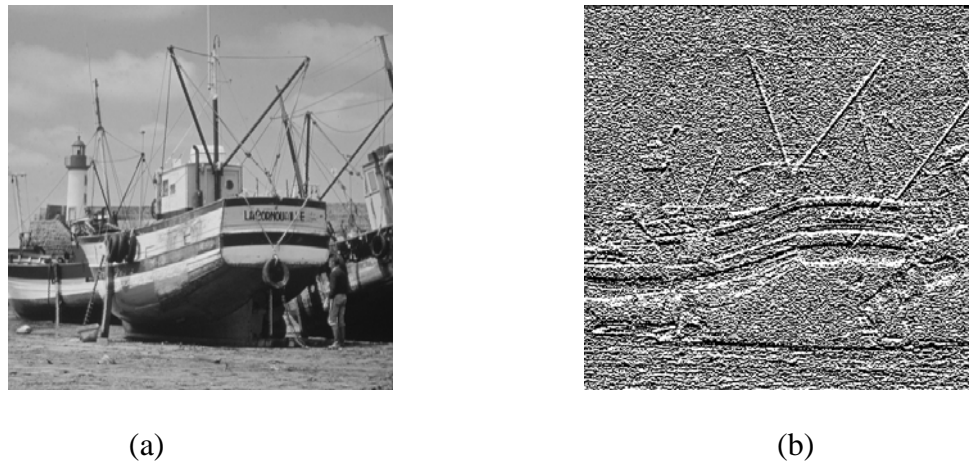


Fig. 3.6 (a) The noisy Boat image and (b) the Sobel processed magnitude gradient image

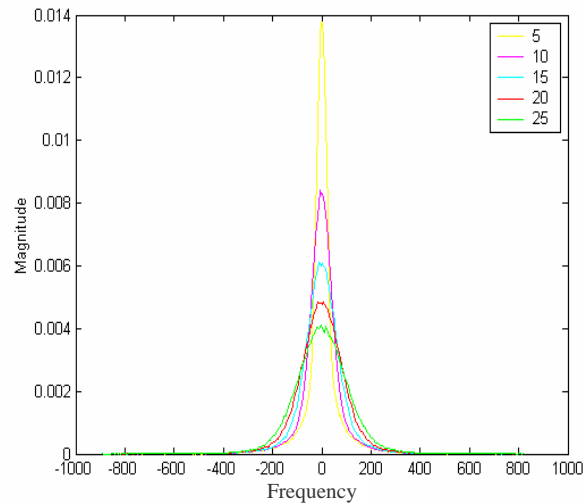


Fig. 3.7 Histogram of the magnitude gradients of the Boat image for varying noise levels by the Sobel operator.

for different noise levels (Gaussian noise, $\sigma_n = 0, 5, 10, 15, 20$), is shown in Fig. 3.7. As can be seen from Fig. 3.7, the curves shift to the right with increasing noise level, i.e., the most frequent magnitude gradient γ moves to the right for higher noise levels.

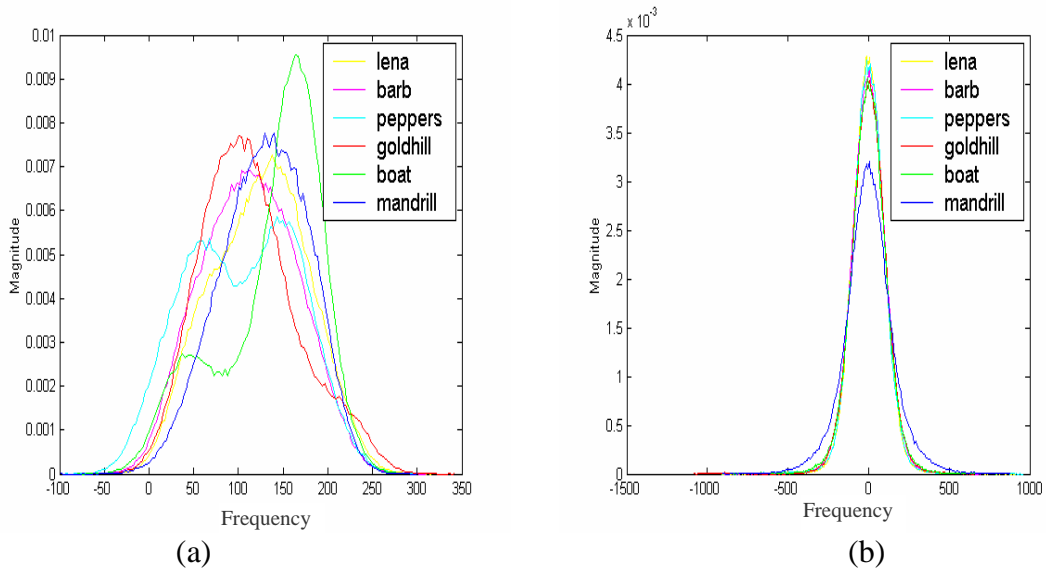


Fig. 3.8 Pixel intensity histogram of the tested noisy images and the corresponding spatial gradient histograms.

The histograms of different images corrupted by the same amount of additive Gaussian noise are in general quite different. This is illustrated for six different images: Lena, Boat, Peppers, Goldhill, Baboon, and Barbara with added Gaussian noise of $\sigma_n = 10$ in Fig. 3.8(a). However, the histograms of the same six images after the Sobel operator has been applied have similar shape and peak at approximately the same abscissa value (see Fig. 3.8(b)).

In many images (except for the highly-textured images and relatively low noise levels) the position of the most frequent gradient γ directly relates to the noise level, i.e., to σ_n . The relationship between the estimated standard deviation σ_e of added Gaussian noise, for an image, and γ can be approximated by the first order Taylor series:

$$\sigma_n = 0.2661\gamma + 0.7827 \quad (3.12)$$

3.3.3 Wavelet-based noise level estimation

A number of wavelet based techniques have been developed for image denoising/enhancement and image coding purposes so the noise estimation methods are preferred in the wavelet domain. The most common approach in this respect is a robust median estimator where the noise standard deviation is estimated as the median absolute deviation (MAD) of the wavelet coefficients in the highest frequency subband divided by 0.6754 [Donoho 1994]. Even though this estimator is expressed by a simple formula, its computation complexity is high due to the sorting operations needed for the median operator. The accuracy of the MAD method of [Donoho 1994] is sensitive to varying noise levels and it also varies for different images.

Wavelet-based noise estimation is a special case of gradient based methods for noise estimation, where the gradient amplitudes are obtained from the corresponding wavelet decomposition subbands, and evaluated in order to obtain the estimated noise variance. Three methods were proposed by Stefano where the results were shown to outperform the MAD method [Stefano 2004]. A first method is a moment matching method, where the noise variance is determined assuming that the noise is additive and Gaussian and that the noise-free image had a Laplacian distribution. Then moments m_2 and m_4 of the noisy image f' (original image f plus noise n) are given by:

$$m_2 = \sigma_f^2 + \sigma_n^2 \quad (3.13)$$

$$m_4 = 6\sigma_f^4 + 3\sigma_n^4 + 6\sigma_f^2\sigma_n^2 \quad (3.14)$$

where σ_f^2 and σ_n^2 stand for the variance of the original f and noisy f' image respectively. The moment matching method utilizes the estimates of the moments, \hat{m}_2

and \hat{m}_4 obtained directly from the image (in the corresponding wavelet band W_n , of the image f'):

$$\hat{m}_k = \frac{1}{N} \sum_{x,y} |W_n(x,y)|^k \quad (3.15)$$

where it is taken into account that the mean value of each wavelet band is zero. Replacing the theoretical moments m_k by their estimates \hat{m}_k and solving equations (3.13 and 3.14) for the unknown noise variance, one obtains the noise estimate as follows:

$$\hat{\sigma}_n = \hat{m}_2 \left(1 - \sqrt{\frac{1}{3} \frac{\hat{m}_4}{\hat{m}_2^2} - 1} \right) \quad (3.16)$$

There are conditions under which the above expression can fail or yield unrealistic values (e.g., when $\hat{m}_4 < 3\hat{m}_2^2$ or $\hat{m}_4 > 6\hat{m}_2^2$). Theoretically, the Gaussian and Laplacian processes, which are used as models for noise and noise-free image respectively, can not produce such cases. However, in practice they do occur because real data does not satisfy the Laplacian model accurately. As a solution, the noise estimate in these cases is put to $\hat{\sigma}_n = \hat{m}_2$ or $\hat{\sigma}_n = 0$, respectively.

The second method called trained moments method, aims at generalizing the moment matching method to avoid the need for assuming a statistical model for the noise-free image and instead employs a training to form a model for an estimate of the noise variance. The algorithm is described in terms of three normalized moments:

$$\begin{aligned} M_1 &= m_1 \\ M_2 &= m_2/m_1 \\ M_4 &= m_4/(m_2m_1) \end{aligned} \quad (3.17)$$

where $M_1 = m_1 = 0$, in case of white Gaussian noise and therefore that component should be excluded from the normalization and the model for noise estimation. The trained

moment matching method assumes no particular distribution of the noise-free image. The only assumption made is that the estimated noise standard deviation $\hat{\sigma}_n$ is a linear combination of the three moments. The aim is to find the best linear model of the moments (M_1 , M_2 and M_3) for the standard deviation of noise $\hat{\sigma}_n$:

$$\hat{\sigma}_n = \alpha_1 M_1 + \alpha_2 M_2 + \alpha_3 M_3 \quad (3.18)$$

The coefficient α_k is determined from a set of training images with different noise levels. The constants α_k are determined by minimizing the mean squared error of the estimated noise variance across the training set of images and across all noise levels.

The third method is a noise estimation method which is based on evaluating the cumulative distribution function (CDF) of the spatially local noise variances. The local variance is determined in terms of the wavelet coefficients and is computed as the sum of squared wavelet coefficients within a local neighborhood.

The local variance is on average the sum of the local noise-free image variance and the noise variance, assuming that the noise and the image are statistically independent. This implies that information about the noise variance can be obtained by examining areas with the smallest values of the local variance. To form a noise estimate based on this information, the cumulative distribution function, $c(q)$, of the local pixel variances is computed. The value of $c(q)$ represents the number of pixels with a local variance less than q . The effectiveness of the method depends upon the choice of the local variance parameter $q = q_0$, which maximizes a discrimination metric evaluated across the training set of images and all the noise levels considered. The mean values of $c(q_0)$ are then computed across the training set of images and are stored for a range of noise variances, in order to form a table of values of $c(q_0)$ versus noise variances. When a new image is

tested, the value of $c(q_0)$ is computed and the noise variance is inferred from the look-up table.

Finally, it should be noted that all wavelet-based methods in this section use only information from the highest frequency (smallest scale) wavelet band. The reason for this is that highest frequency band from a first scale has the smallest Signal to Noise Ratio (SNR).

3.4 EXPERIMENTAL RESULTS AND DISCUSSION

In this section, two simple, yet reliable methods for estimating the noise variance from the noisy image are implemented. The first method is block-based estimation of noise in the noisy image as discussed in 3.3.1. It is assumed that an image has many regions of almost uniform intensity and that most changes in these regions of insignificant variations are due to the noise. This assumption is generally valid for many real-world images. The background of a scene is an example of such a region of insignificant variations. Also the noise n is assumed to have a constant variance σ_n^2 throughout the image. This is a direct consequence of the fact that the noise is assumed to be a i.i.d. Gaussian process. The local variance estimates of all window masks of size $N \times N$ pixels, centered at every pixel of the image, are then calculated. The choice of the window size over which to estimate the local variance is important. It needs to be at least 5×5 for reasonable noise estimates, but it should also be small enough to ensure local signal stationarity. Experimentally, it was observed that both 5×5 and 7×7 work well but latter yields better results. Fig. 3.9 illustrates the histogram of these local variance estimates in Lena image with noise standard deviation of 25. Examining the distribution of the local variance across the entire image and assuming that most of the local 7×7 sub-

regions of the image have insignificant signal variations. The mode (i.e. the most frequent value) of the local variance distribution (histogram) was shown to be a reasonable estimator of the noise variance [Gonzalez 2000] and [Sonka 1999]. This strategy yields the following estimate of the noise variance:

$$\hat{\sigma}_n^2 = 636 \text{ or } \hat{\sigma}_n = 25.22 \quad (3.17)$$

which is relatively close to the true noise standard deviation $\sigma_n = 25$.

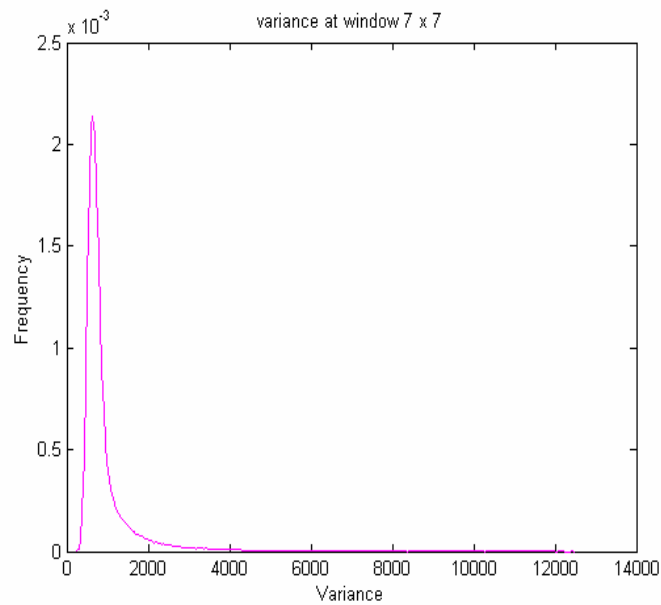


Fig. 3.9 The histogram of local noise variance of noisy Lena Image

The second method is based on wavelet. The method is used for noise estimation in latter chapters because the processing is in same domain. The basic concepts of DWT of an image are used here. Recall that the wavelet decomposition of an image is done as follows: In the first level of decomposition, the image is split into four subbands, namely A_1 , H_1 , V_1 , and D_1 . The D_1 sub-band gives the diagonal details of the image; the H_1 subband gives the horizontal details, while the V_1 represents the vertical details. The A_1

subband is the low resolution residual consisting of low frequency components and this subband is further split at higher levels of decomposition. It has been shown that the noise standard deviation σ_n can be accurately estimated from the diagonal subband D_1 of first decomposition level by the robust and accurate median estimator [Donoho 1994], as given by

$$\hat{\sigma}_n = \frac{\text{median}(|D_1|)}{0.6745} \quad (3.18)$$

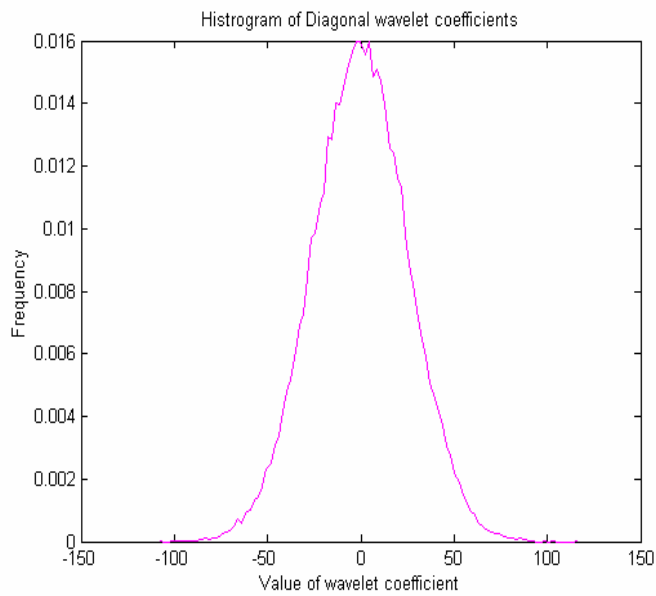


Fig. 3.10 The histogram of wavelet coefficients of diagonal subband D_1 .

Although the original image is responsible for a few large amplitude outliers, these few coefficients have little impact on the median operator. Fig. 3.10 illustrates the distribution of the wavelet coefficients in the first level diagonal subband, D_1 of the wavelet coefficients.

Note that this distribution is highly symmetric, with zero mean and resembles a Gaussian distribution. Table 3.1 illustrates the statistics as well as the estimate of the noise standard

deviation σ_n . Clearly, for the test image of Lena with true noise standard deviation $\sigma_n = 25$, a very accurate estimate ($\hat{\sigma}_n = 25.015$) is obtained. The wavelet-based method yields the best estimate of the noise variance among the two implemented methods. This is because the discrete wavelet transform performs a significant degree of localization both spatially and in frequency. Consequently, in the subband D_1 , most of the wavelet coefficients are due to noise. Although, the original image is responsible for a few large amplitude outliers, these few coefficients have little impact on the median operator. In what follows, this wavelet-based method will be adopted as the method of choice and the noise intensity will be estimated by

$$\sigma_n \approx \hat{\sigma}_n = 25.015 \quad (3.19)$$

Table 3.1
The estimated noise for Lena image

Size of D_1	Mean (D_1)	Variance(D_1)	Std(D_1)	Median($ D_1 $)	$\hat{\sigma}_n = \frac{\text{median}(D_1)}{0.6745}$	Absolute Error E
256 x 256	0.000	614.598	25.330	17.012	25.015	0.015

3.5 SUMMARY

In this chapter, different noise estimation methods are studied in spatial domain and wavelet domain. The noise estimation is important step of image denoising for optimal performance of algorithms. The noise variance is used as a parameter in shrinkage function. Two methods are implemented in this chapter; one is block-based and other is wavelet-based for Gaussian additive noise. The wavelet-based method is better than block-based method in accuracy and processing. It is used in latter chapters to estimate noise.